



CHORUS

This is the accepted manuscript made available via CHORUS. The article has been published as:

Entanglement Hamiltonian of Many-Body Dynamics in Strongly Correlated Systems

W. Zhu, Zhoushen Huang, Yin-Chen He, and Xueda Wen

Phys. Rev. Lett. **124**, 100605 — Published 13 March 2020

DOI: [10.1103/PhysRevLett.124.100605](https://doi.org/10.1103/PhysRevLett.124.100605)

Entanglement Hamiltonian of Many-body Dynamics in Strongly-correlated Systems

W. Zhu¹, Zhoushen Huang², Yin-Chen He³, and Xueda Wen⁴

¹*Institute of Natural Science, Westlake Institute of Advanced Study and School of Science, Westlake University, Hangzhou, 310024, China*

²*Argonne National Laboratory, Lemont, IL 60439, USA*

³*Perimeter Institute for Theoretical Physics, Waterloo, Ontario N2L 2Y5, Canada and*

⁴*Department of Physics, Massachusetts Institute of Technology, Cambridge, MA 02139, USA*

A powerful perspective in understanding non-equilibrium quantum dynamics is through the time evolution of its entanglement content. Yet apart from a few guiding principles for the entanglement entropy, to date, much less is known about the refined characteristics of entanglement propagation. Here, we unveil signatures of the entanglement evolving and information propagating out-of-equilibrium, from the view of the entanglement Hamiltonian. We investigate quantum quench dynamics of prototypical Bose-Hubbard model using state-of-the-art numerical technique combined with conformal field theory. Before reaching equilibrium, it is found that a current operator emerges in the entanglement Hamiltonian, implying that entanglement spreading is carried by particle flow. In the long-time limit the subsystem enters a steady phase, evidenced by the dynamic convergence of the entanglement Hamiltonian to the expectation of a thermal ensemble. Importantly, the entanglement temperature in steady state is spatially independent, which provides an intuitive trait of equilibrium. These findings not only provide crucial information on how equilibrium statistical mechanics emerges in many-body dynamics, but also add a tool to exploring quantum dynamics from the perspective of the entanglement Hamiltonian.

Introduction.— The power of classical statistical mechanics is rooted in the ergodic hypothesis, but in closed quantum many-body systems, how “memories” are forgotten in a realistic time scale [1–4] — how steady states and thermal behavior at later times emerge dynamically [5–7]— remains an actively investigated topic [8–11]. Motivated by significant progress in experimental techniques that have made the dynamics of quantum systems accessible [12–22], a recent surge of theoretical interest has focused on the problem of non-equilibrium quantum dynamics. In many cases, particularly in interacting systems, to directly access such dynamics remains technically challenging due to the increasing amount of correlations generated over time [23, 24].

From an entanglement point of view, these correlations are a consequence of entangled quasiparticle pairs being constantly generated and propagating into different parts of the system [23–28]. The dynamics of these quasiparticles have been shown to reflect the underlying nature of their hosting systems, e.g., ballistic in thermalizing systems [25, 29–31] versus logarithmic in localized systems [32–35]. In many of these examples, propagation of entanglement also spreads conserved quantities which can serve as information carriers [23, 36–38]. An important aspect to understanding quantum dynamics and the emergence of equilibration is therefore to understand the dynamics of quantum entanglement [10], even in systems without identifiable quasiparticle content [30, 39–42]. In this context, entanglement dynamics is also connected with information loss and scrambling [43–48].

In equilibrium condensed matter systems, entanglement-based analysis has already proved to be a profitable tool as a diagnostic of strong correlations, from the presence of topological order to the onset of quantum criticality [49]. Indeed, the scaling of entanglement entropy characterizes the quantum statistics of quasiparticles [50, 51], and entanglement spectrum encompasses a direct relation between bulk

and edge physics [52], both of which highlight the wealth of information encoded in entanglement. While entanglement entropy and entanglement spectrum are important measures of quantum information, the entanglement Hamiltonian (EH) is a more fundamental object. The EH is a sum of the local “energy” density $\mathcal{H}(x)$ weighted by a local inverse of entanglement temperature $\beta(x)$: $H_E = \int dx \beta(x) \mathcal{H}(x)$. The relationship between EH and the reduced density matrix of a subsystem (A), $\rho_A = e^{-H_E}$, implies that ρ_A can be interpreted as a canonical ensemble with energy density $\mathcal{H}(x)$ in local thermal equilibrium at temperature $\beta^{-1}(x)$ [53]. Therefore, knowledge of the EH could offer an alternative picture of how subsystem A behaves by appealing to our thermodynamic intuition. However, precise knowledge about the EH is rare, even for static systems [54, 55]. Recently, numerical efforts have attempted to obtain the EH in static interacting systems using various methods [56–58], and have shed some light on this technically challenging problem. As for time-evolving systems, although results for non-interacting cases have been obtained [59–63], the quantitative role of EH in strongly-correlated systems remains unexplored, and it is highly desirable to systematically study the time dependence of EH.

In this work, we study the EH in the quench dynamics of the Bose Hubbard model, a prototypical non-integrable system, based on the time-dependent density-matrix renormalization group (t-DMRG) approach [64, 65]. With the help of a recently developed numerical scheme [58], we are able to track the time dependence of the EH in real time. Our main findings are that: 1) a current operator emerges in the EH before the system reaches equilibrium, reflecting the propagation of entanglement carried by particle flow; 2) in the long-time limit, the EH becomes nearly stationary and demonstrates features of equilibrium; 3) the steady state exhibits a spatially independent entanglement temperature, signaling the subsystem

becomes locally thermalized. These results are endorsed by the conformal field theory (CFT). These findings imply that the EH can be used to effectively investigate the emergence of subsystem equilibrium under the unitary dynamics of the full system, which sets up a valuable paradigm for exploring entanglement dynamics out-of-equilibrium.

Preliminary.— We begin by discussing the salient features of the EH dynamics after a quantum quench, in the framework of 1+1D CFT. We consider a 1D chain with finite length L defined on $x \in [0, L]$, and the subsystem A under consideration is chosen as $[0, l]$. At time $t = 0$, we start from an initial state with short-range entanglement, which may be considered as the ground state of a gapped Hamiltonian. At $t > 0$ we evolve it with a CFT Hamiltonian $H_{\text{CFT}} = \int dx \mathcal{H}(x)$. We consider the “semi-infinite” condition ($l \ll L$), where the other boundary at $x = L$ can be safely neglected when we focus on the subsystem $A = [0, l]$.

Based on conformal mappings, we obtained the exact form of the EH (See supplementary materials for details [66]). Importantly, we found that in the long-time limit, the EH of subsystem A is the sum of $\mathcal{H}(x)$ weighted by a spatially dependent finite temperature $\beta^{-1}(x)$, indicating that the reduced density matrix $\rho_A(t)$ takes the form of a thermal ensemble. To be specific, in the long time limit $t \gg l$, one obtains the EH $H_E = \int dx \beta(x) \mathcal{H}(x)$, with the envelope function [66]

$$\beta(x) = 2\beta_0 \cdot \frac{\sinh(\pi(l+x)/\beta_0) \sinh(\pi(l-x)/\beta_0)}{\sinh(2\pi l/\beta_0)}, \quad (t \gg l). \quad (1)$$

Here β_0 characterizes the correlation length of the gapped pre-quench state [27], and it also qualifies the effective “temperature” of energy density of the system using pre-quench state [66]. In addition, as notable byproducts, CFT also gives time dependence of entanglement entropy to the leading order [25, 26, 66]:

$$S(t) = \begin{cases} \frac{3c}{\pi\beta_0} t, & t < l \\ \frac{3c}{\pi\beta_0} l, & t > l \end{cases}, \quad (2)$$

where c is the central charge of the underlying CFT. That is, the entanglement entropy grows linearly in time until it saturates at a value satisfying the volume law [66].

Model and Method.— We now turn to a paradigmatic non-integrable model, the one-dimensional Bose-Hubbard model, which has been experimentally realized with ultracold gases in deep optical lattices [67],

$$\hat{H} = -J \sum_i (b_i^\dagger b_{i+1} + h.c.) + \frac{U}{2} \sum_i n_i(n_i - 1), \quad (3)$$

where b_i^\dagger (b_i) is the boson creation (annihilation) operator and $n_j = b_j^\dagger b_j$ is the on-site density operator. Throughout this work, we consider a uniform Hamiltonian density, i.e. the physical coupling J (set to $J = 1$) and interaction U are spatially independent. In the equilibrium case, at fixed filling $\langle n_i \rangle = 1$, a critical value $U_c \approx 3.38$ [68, 69] separates

a Mott insulating phase ($U > U_c$) from a superfluid phase ($U < U_c$), the latter described by an effective Luttinger liquid theory with $c = 1$. Below we set the initial state in the Mott phase as the ground state of H with pre-quench condition $U^i > U_c$, and investigate its quench dynamics under the H with post-quench condition $U^f < U_c$.

To simulate the unitary time evolution $|\Psi(t)\rangle = \mathcal{U}(t)|\Psi(t=0)\rangle$, we use the time-dependent density-matrix renormalization group (t-DMRG) [64, 65]. We apply a second-order Trotter decomposition of the short time propagator $\mathcal{U}(\Delta t) = \exp(-i\Delta t \hat{H})$ into a product of terms which acts only on two nearest-neighbor sites. We use a dimension up to 5120, which guarantees that the neglected weight in the Schmidt decomposition in each time step is less than 10^{-6} . Once the $|\Psi(t)\rangle$ is computed, we partition the one-dimensional chain of length L into two segments, ℓ and $L - \ell$, and calculate the subsystem reduced density matrix, $\rho_\ell(t) = \text{Tr}_{L-\ell} |\Psi(t)\rangle \langle \Psi(t)|$. The entanglement Hamiltonian is formally defined as $\rho_A(t) = \exp(-\hat{H}_E)$, but it is technically challenging to extract \hat{H}_E through this definition because the transformation $\hat{H}_E(t) = -\ln \rho_A(t)$ is non-linear. Very recently, a generic scheme to obtain the operator form of EH has been proposed in Ref. [58], which we briefly outline here. The starting point is to define a set of basis operators \hat{L}_a , which we take as the boson hopping operator $b_i^\dagger b_j$ and density interaction operator $n_i(n_i - 1)$ according to the form of the physical Hamiltonian. These operators define the variational space in which we search for the “best” EH in the form $H_E = \sum_a w_a \hat{L}_a$, where w_a are parameters coupled to operators \hat{L}_a . Practically, the variational scheme is equivalent to solving the eigenvalue problem of the correlation matrix $G_{ab} = \langle \xi | \hat{L}_a \hat{L}_b | \xi \rangle - \langle \xi | \hat{L}_a | \xi \rangle \langle \xi | \hat{L}_b | \xi \rangle$ [58, 70, 71], where $|\xi\rangle$ is a reference state chosen here as one eigenstate of ρ_A . The lowest eigenvalue of G_{ab} , i.e. g_0 , minimizes the variance $\langle \xi | H_E^2 | \xi \rangle - \langle \xi | H_E | \xi \rangle^2$, which can be interpreted as the “fluctuation” of “Hamiltonian” $H_E = \sum_a w_a \hat{L}_a$ under $|\xi\rangle$. The eigenvector of g_0 gives rise to the estimate of $\{w_a\}$. It has

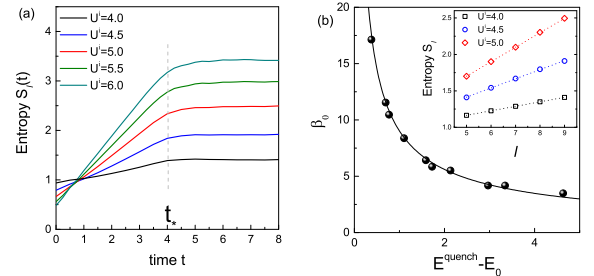


FIG. 1: Dynamics of the entanglement entropy. (a) Time-evolution of entanglement entropy by quenching from various U^i to $U^f = 3.3$. (b) Effective inverse of temperature β_0 as a function of $E^{\text{quench}} - E_0$, where E_0 is the lowest energy of post-quench Hamiltonian $\hat{H}(U^f)$ and $E^{\text{quench}} = \langle \Psi(t=0) | H(U^f) | \Psi(t=0) \rangle$. The black line is the best fit to $\beta_0 \propto (E^{\text{quench}} - E_0)^\alpha$, $\alpha = -0.641 \pm 0.012$. Inset: Linear scaling of $S_\ell = \frac{\pi c}{3\beta_0} \ell$ to the length of the subsystem ℓ .

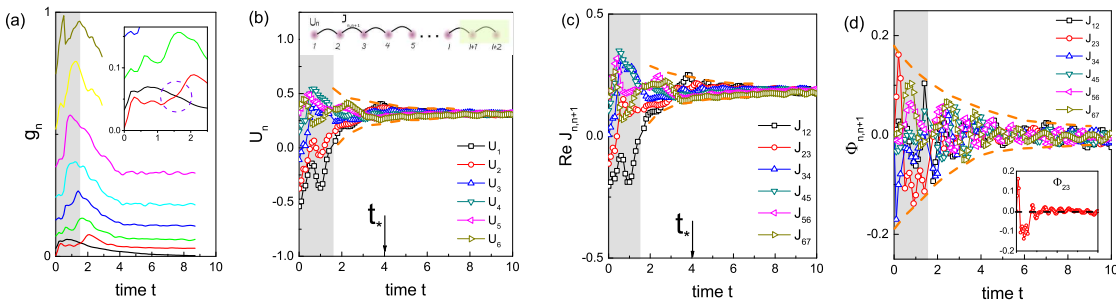


FIG. 2: **Dynamics of the EH.** (a) Spectrum of correlation matrix $G_{ab}(t)$. The lowest and second lowest eigenvalue crosses with each other at $t_0 \approx 1.65$ (inset). The shaded area shows the short time regime $t < t_0$. The parameters of the EH (see Eq. 4) as a function of time: (b) interaction strength $U_n(t)$, (c) real part of couplings $Re J_{n,n+1}(t)$, (d) relative phase of couplings $\Phi_{n,n+1}(t) = \arg J_{n,n+1}$, where n labels spatial lattice sites. Here we quench the Bose-Hubbard model (Eq. 3) from $U^i = 5.0$ to $U^f = 3.3$. The total system size $L = 48$ and the typical subsystem length is $\ell = 9$. Different symbols label local coupling and interaction strengths. The brown dashed line is guide to eye. Inset of (b) is the cartoon picture of one dimension chain and entanglement bipartition.

been confirmed that [58], in the static case, this numerical receipt can give reliable EH that faithfully captures all features of the reduced density matrices. In this work, we generalize and formulate this scheme using the matrix-product state ansatz, which is amenable to simulating the time evolution of the EH within the t-DMRG approach, and works well for larger system sizes compared to exact diagonalization.

Entanglement entropy.— We compute the time-dependent entanglement entropy and compare with the CFT results obtained earlier. Fig. 1(a) shows the time evolution of the entanglement entropy for various initial conditions U^i . For all cases, $S_\ell(t)$ shows two temporal regimes: At short times $t < t_*$, the entropy exhibits a linear rise, until it bends over to an almost flat plateau. The linear increase can be accounted for by the “ballistic” propagation of entanglement. At long times $t > t_*$, the entropy saturates to its steady-state value. As shown in inset of Fig. 1(b), the saturation of the entropy depends linearly on the block length, which clearly exhibits a “volume-law” scaling. In particular, based on the relationship of Eq. 2, we can extract the pre-quench parameter β_0 (or the inverse of entanglement temperature) In Fig. 1(b), we show the dependence of β_0 on the post-quench energy above the ground state, $E^{\text{quench}} - E_0$, where E^{quench} is the energy of the pre-quench state in the post-quench Hamiltonian, and E_0 is the post-quench ground state energy. It is clear that β_0 monotonically decreases with $E^{\text{quench}} - E_0$. Our best fitting gives the scaling $\beta_0 \propto (E^{\text{quench}} - E_0)^\alpha$, $\alpha \approx -0.641 \pm 0.012$. It reflects that a higher initial energy translates to a higher effective temperature.

Entanglement Hamiltonian.— Next we turn to discuss the time evolution of EH. Here we assume the EH has following form (detailed discussion see [66]):

$$H_E(t) = - \sum_i (J_{i,i+1}(t) b_i^\dagger b_{i+1} + h.c.) + \sum_i \frac{U_i(t)}{2} n_i(n_i - 1). \quad (4)$$

We map out the EH at each time step by using the scheme described in the method section [58]. Fig. 2(a) shows the

spectrum of correlation matrix as a function of time. Interestingly, there is a level crossing between the lowest and second lowest eigenvalue around $t_0 \approx 1.65$ (inset of Fig. 2). After this critical time, the lowest eigenvalue g_0 monotonically decreases, which implies the trial EH works better in the time regime $t > t_0$. Next we will focus on the $t > t_0$ regime and discuss the salient features of the EH.

Fig. 2(b-c) shows the time evolution of the interaction strength $U_i(t)$, and the real part of the coupling strength $Re J_{i,i+1}(t)$ after a global quench. First, both J and U show sizable oscillations at early times $t < t_0$, and later the subsequent dynamics gradually reduce (as indicated by the dashed curve envelope). In particular, in the long-time limit $t > t_*$, all coupling strengths approach nearly stationary values. Physically, this suggests the subsystem has equilibrated to a steady state.

Second, before reaching equilibrium, it is found the imaginary part of boson hopping strength is nonzero. To show this, we define the phase angle $\Phi_{i,i+1} = \arg J_{i,i+1} = \tan^{-1} \frac{Im J_{i,i+1}}{Re J_{i,i+1}}$, and the phase angle directly relates to the imaginary part of coupling strength $Im J_{i,i+1}(t) = |J_{i,i+1}| \sin \Phi_{i,i+1}$. In Fig. 2(d), $\Phi_{i,i+1}(t > 0)$ shows oscillation behaviors due to the non-equilibrium dynamics. For comparison, in the static case we have $\Phi_{i,i+1}(t = 0) = 0$. Since $Im J_{i,i+1}$ is directly coupled to the current operator $\hat{J}_c = i[H, x] = i \sum_i (b_n^\dagger b_{n+1} - b_n b_{n+1}^\dagger)$ (we set $e = \hbar = 1$), this implies that time-reversal symmetry is broken, and a non-vanishing particle current flow emerges in time evolution. The emergent current flow reflects quasiparticle propagation, which is consistent with the picture that quasiparticles serve as entanglement information carriers[25]. The inset of Fig. 2(d) single out one typical evolution ($\Phi_{2,3}$). It signals that the current first flows from the entanglement cut into the bulk ($\Phi_{2,3} > 0$), and then reverse direction ($\Phi_{2,3} < 0$), and reduces to zero in the long time. This again shows the transport of quasiparticles. At long times, the imaginary part tends to vanish with only small fluctuations around zero, suggesting that the subsystem has reached equilibrium and net particle flow is

absent. The appearance of current in the EH allows us to conclude that information spreading originates in the propagation of quasiparticles between the two bipartition constituents [25].

Third, as shown in Fig. 2(b-c), in the long time limit $t > t_*$ the evolution of local coupling and interaction strengths at different spatial locations tend to converge to the same value, indicating that the EH is spatially uniform away from the entanglement cut. To further study the spatial dependence of the EH at the long-time limit, we plot the effective inverse of temperature $\beta(x)/\beta_0$ (equivalent to time-averaged local coupling strengths) in Fig. 3. In Fig. 3(a), we show the spatial dependence of inverse entanglement temperature in the long time limit. In particular, local temperatures are nearly uniformly distributed away from the entanglement cut ($x \ll \ell$). Crucially, this spatial dependence shows excellent agreement with the CFT prediction Eq. (1). Moreover, we demonstrate that the residual fluctuations near the entanglement cut $x \sim \ell$ can be interpreted as a finite (initial) temperature effect. In Fig. 3(b), we show that by increasing initial temperature (through changing quenching parameters as discussed in Fig. 1(b)), the spatial independence of long-time entanglement temperatures becomes sharper near the entanglement cut $x \sim \ell$. The consistency with the CFT Eq. (1) indicates that local temperatures should be completely flat (shown by dashed line) when $\beta_0 \rightarrow 0$ (infinite initial temperature limit), which is also supported by our numerical results (inset of Fig. 3(b)).

Lastly, we stress that, the above findings offer an intuitive trait of equilibrium. Physically, at the finite initial temperature, the obtained local entanglement temperature $\beta^{-1}(x)$ indicates that the equilibrium of a physical subsystem A depends on distance from a “heat source” that is subsystem \bar{A} . In the infinite temperature limit, the entanglement temperature in steady state is spatially independent. From this point of view, it is appealing that a spatially independent $\beta(x)$ reveals the local temperature reaches the effective equilibrium.

Summary and Discussion.— We have addressed the out-of-equilibrium dynamics of strongly-correlated systems from the point of view of the entanglement Hamiltonian. By tracking the time evolution of the entanglement Hamiltonian, we were able to gain remarkable signatures of the entanglement propagation and information scrambling. We demonstrate that, the entanglement Hamiltonian involves an emergent current operator which drives the quasiparticle propagation towards equilibrium. In the long-time limit the entanglement Hamiltonian becomes stationary. In particular, spatially distributed entanglement temperature satisfies a universal feature as proposed by conformal field theory, indicating the subsystem indeed reaches equilibrium away from the entanglement cut. Our results show that the entanglement Hamiltonian provides fundamental insight into the non-equilibrium dynamics of quantum many-body systems.

To our knowledge, the effective temperature in a driven quantum system has not been explored in numerical calculations. Yet it is unclear how one may infer a meaningful “temperature” in the study of non-equilibrium problems in quantum many-body systems. Here, our numerical framework

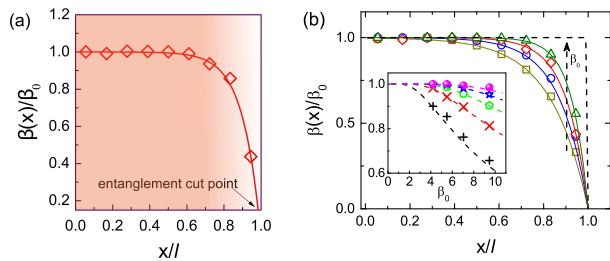


FIG. 3: Spatial dependence of the local entanglement temperature. (a) Local inverse of temperature $\beta(x)/\beta_0$ at long time limit (red diamonds) and related fitting (red line) to envelope function Eq. (1). The background color shows gradient map of the inverse of temperature. (b) Spatial dependence of local inverse of temperature for various initial condition β_0 . The different β_0 is achieved by varying quenching parameters (see Fig. 1(b)): $U^i = 4.0, U^f = 3.3$ (yellow squares), $U^i = 4.5, U^f = 3.3$ (blue circles), $U^i = 5.0, U^f = 3.3$ (red diamonds) and $U^i = 5.5, U^f = 3.3$ (green triangles). The solid lines show best fit to the envelope function Eq. (1). Inset: Effective temperature scaling to infinite initial temperature limit ($\beta_0 \rightarrow 0$).

provides a natural way to identify the effective “temperature” of a subsystem and its dynamical evolution toward equilibrium, thus it allows for a direct measure of local temperatures coming from the individual degrees of freedom enclosed in subsystem.

In closing, we would like to make several remarks. Although the limited system sizes prevent comparison over a large range of subsystem sizes, we confirm the characteristics of entanglement Hamiltonian with underlying scaling behavior are robust on all system sizes that we can reach [66]. Moreover, we investigated numerically a variety of one-dimensional systems of different kinds [66]. Through these studies, our results have implications well beyond the specific model. Lastly, our findings open up several avenues for future investigation. For instance, applying these tools for characterizing the presence of equilibrium could be powerful in studying many-body localization [8, 10, 77], where one of the key features is the suppression of entanglement. In addition, taking into account the recent proposal in synthetic quantum systems [78], the dynamics of constructed entanglement Hamiltonian may be valuable for future experiments.

Acknowledgments.— W.Z. thanks Beni Yoshida, M. Dalmonte, E. Tonni for discussion, Michael Reed for a critical proof-reading of the final manuscript. This work was supported by the start-up funding at Westlake University and project 11974288 supported by NSFC. Work at Argonne was supported by ANL LDRD Proj. 1007112. X.W. is supported by the Gordon and Betty Moore Foundations EPiQS initiative through Grant No.GBMF4303 at MIT. Research at Perimeter Institute (YCH) is supported by the Government of Canada through the Department of Innovation, Science and Economic Development Canada and by the Province of Ontario through the Ministry of Research, Innovation and Science.

-
- [1] L. D'Alessio, Y. Kafri, and M. Polkovnikov, A. Rigol, *Advances in Physics* **65**, 239 (2016).
- [2] T. Mori, T. N. Ikeda, E. Kaminishi, and M. Ueda, *Journal of Physics B: Atomic, Molecular and Optical Physics* **51**, 112001 (2018), URL <https://doi.org/10.1088/2F1361-6455%2Faabcdf>.
- [3] F. Borgonovi, F. Izrailev, L. Santos, and V. Zelevinsky, *Physics Reports* **626**, 1 (2016), ISSN 0370-1573, quantum chaos and thermalization in isolated systems of interacting particles, URL <http://www.sciencedirect.com/science/article/pii/S0370157316000831>.
- [4] C. Gogolin and J. Eisert, *Reports on Progress in Physics* **79**, 056001 (2016), URL <https://doi.org/10.1088/2F0034-4885%2F79%2F5%2F056001>.
- [5] J. M. Deutsch, *Phys. Rev. A* **43**, 2046 (1991), URL <https://link.aps.org/doi/10.1103/PhysRevA.43.2046>.
- [6] M. Srednicki, *Phys. Rev. E* **50**, 888 (1994), URL <https://link.aps.org/doi/10.1103/PhysRevE.50.888>.
- [7] M. Rigol, V. Dunjko, and M. Olshanii, *Nature* **452**, 854 (2008), URL <https://doi.org/10.1038/nature06838>.
- [8] R. Nandkishore and D. A. Huse, *Annual Review of Condensed Matter Physics* **6**, 15 (2015).
- [9] J. M. Deutsch, *Reports on Progress in Physics* **81**, 082001 (2018), URL <https://doi.org/10.1088/2F1361-6633%2Faac9f1>.
- [10] D. A. Abanin, E. Altman, I. Bloch, and M. Serbyn, *Rev. Mod. Phys.* **91**, 021001 (2019), URL <https://link.aps.org/doi/10.1103/RevModPhys.91.021001>.
- [11] A. Polkovnikov, K. Sengupta, A. Silva, and M. Vengalattore, *Rev. Mod. Phys.* **83**, 863 (2011), URL <https://link.aps.org/doi/10.1103/RevModPhys.83.863>.
- [12] J. Eisert, M. Friesdorf, and C. Gogolin, *Nature Physics* **83**, 863 (2015), URL <https://doi.org/10.1038/nphys3215>.
- [13] S. Trotzky, Y. A. Chen, A. Flesch, I. P. McCulloch, U. Schollwöck, J. Eisert, and I. Bloch, *Nature Physics* **8**, 325 (2012).
- [14] P. Jurevic, B. P. Lanyon, P. Hauke, C. Hempel, P. Zoller, R. Blatt, and C. F. Roos, *Nature* **511**, 202 (2014), URL <https://doi.org/10.1038/nature13461>.
- [15] P. Richerme, Z. X. Gong, A. Lee, C. Senko, J. Smith, M. Foss-Feig, M. S., A. V. Gorshkov, and C. Monroe, *Nature* **511**, 198 (2014), URL <https://doi.org/10.1038/nature13450>.
- [16] C. Neill, P. Roushan, M. Fang, Y. Chen, M. Kolodrubetz, Z. Chen, A. Megrant, R. Barends, B. Campbell, B. Chiaro, et al., *Nature Physics* **12**, 1037 (2016).
- [17] S. Choi, J. Choi, R. Landig, G. Kucsko, H. Zhou, J. Isoya, F. Jelezko, S. Onoda, H. Sumiya, V. Khemani, et al., *Nature* **543**, 221 (2017), URL <https://doi.org/10.1038/nature21426>.
- [18] H. Bernien, S. Schwartz, A. Keesling, H. Levine, A. Omran, H. Pichler, S. Choi, A. S. Zibrov, M. Endres, M. Greiner, et al., *Nature* **551**, 579 (2017), URL <https://doi.org/10.1038/nature24622>.
- [19] J. Zhang, G. Pagano, P. W. Hess, A. Kyprianidis, P. Becker, H. Kaplan, A. V. Gorshkov, Z.-X. Gong, and C. Monroe, *Nature* **551**, 601 (2017), URL <https://doi.org/10.1038/nature24654>.
- [20] A. M. Kaufman, M. E. Tai, A. Lukin, M. Rispoli, R. Schittko, P. M. Preiss, and M. Greiner, *Science* **353**, 794 (2016), URL <https://doi.org/10.1126/science.aaf6725>.
- [21] M. Greiter, V. Schnells, and R. Thomale, *Phys. Rev. B* **98**, 081113 (2018), URL <https://link.aps.org/doi/10.1103/PhysRevB.98.081113>.
- [22] Y. Tang, W. Kao, K.-Y. Li, S. Seo, K. Mallayya, M. Rigol, S. Gopalakrishnan, and B. L. Lev, *Phys. Rev. X* **8**, 021030 (2018), URL <https://link.aps.org/doi/10.1103/PhysRevX.8.021030>.
- [23] E. H. Lieb and D. W. Robinson, *Comm. Math Phys.* **28**, 251 (1972).
- [24] B. Nachtergaele, Y. Ogata, and R. Sims, *Journal of Statistical Physics* **124**, 1 (2006), ISSN 1572-9613, URL <https://doi.org/10.1007/s10955-006-9143-6>.
- [25] P. Calabrese and J. Cardy, *Journal of Statistical Mechanics: Theory and Experiment* **2005**, P04010 (2005), URL <http://stacks.iop.org/1742-5468/2005/i=04/a=P04010>.
- [26] P. Calabrese and J. Cardy, *Phys. Rev. Lett.* **96**, 136801 (2006), URL <https://link.aps.org/doi/10.1103/PhysRevLett.96.136801>.
- [27] P. Calabrese and J. Cardy, *Journal of Statistical Mechanics: Theory and Experiment* **2016**, 064003 (2016), URL <https://doi.org/10.1088/2F1742-5468%2F2016%2F06%2F064003>.
- [28] M. B. Hastings, arXiv e-prints arXiv:1008.5137 (2010), 1008.5137.
- [29] G. D. Chiara, S. Montangero, P. Calabrese, and R. Fazio, *Journal of Statistical Mechanics: Theory and Experiment* **2006**, P03001 (2006), URL <http://stacks.iop.org/1742-5468/2006/i=03/a=P03001>.
- [30] H. Kim and D. A. Huse, *Phys. Rev. Lett.* **111**, 127205 (2013), URL <https://link.aps.org/doi/10.1103/PhysRevLett.111.127205>.
- [31] H. Casini and M. Huerta, *Journal of Physics A: Mathematical and Theoretical* **42**, 504007 (2009), URL <https://doi.org/10.1088/2F1751-8113%2F42%2F50%2F504007>.
- [32] J. H. Bardarson, F. Pollmann, and J. E. Moore, *Phys. Rev. Lett.* **109**, 017202 (2012), URL <https://link.aps.org/doi/10.1103/PhysRevLett.109.017202>.
- [33] F. Igłó, Z. Szatmári, and Y.-C. Lin, *Phys. Rev. B* **85**, 094417 (2012), URL <https://link.aps.org/doi/10.1103/PhysRevB.85.094417>.
- [34] C. K. Burrell and T. J. Osborne, *Phys. Rev. Lett.* **99**, 167201 (2007), URL <https://link.aps.org/doi/10.1103/PhysRevLett.99.167201>.
- [35] M. Serbyn, Z. Papić, and D. A. Abanin, *Phys. Rev. Lett.* **110**, 260601 (2013), URL <https://link.aps.org/doi/10.1103/PhysRevLett.110.260601>.
- [36] X.-L. Qi and A. Streicher, arXiv e-prints arXiv:1810.11958 (2018), 1810.11958.
- [37] V. Alba and P. Calabrese, *Proceedings of the National Academy of Sciences* **114**, 7947 (2017), URL <https://doi.org/10.1073/pnas.1703516114>.
- [38] A. Nahum, J. Ruhman, S. Vijay, and J. Haah, *Phys. Rev. X* **7**, 031016 (2017), URL <https://link.aps.org/doi/10.1103/PhysRevX.7.031016>.

- [39] A. M. Luchli and C. Kollath, *Journal of Statistical Mechanics: Theory and Experiment* **2008**, P05018 (2008), URL <https://doi.org/10.1088%2F1742-5468%2F2008%2F05%2Fp05018>.
- [40] R. Pal and A. Lakshminarayan, *Phys. Rev. B* **98**, 174304 (2018), URL <https://link.aps.org/doi/10.1103/PhysRevB.98.174304>.
- [41] H. Liu and S. J. Suh, *Phys. Rev. Lett.* **112**, 011601 (2014), URL <https://link.aps.org/doi/10.1103/PhysRevLett.112.011601>.
- [42] H. Casini, H. Liu, and M. Mezei, *Journal of High Energy Physics* **2016**, 77 (2016), ISSN 1029-8479, URL [https://doi.org/10.1007/JHEP07\(2016\)077](https://doi.org/10.1007/JHEP07(2016)077).
- [43] P. Hosur, X. Qi, D. Roberts, and B. Yoshida, *J. High Energ. Phys.* **2016** (2016), URL [https://doi.org/10.1007/JHEP02\(2016\)004](https://doi.org/10.1007/JHEP02(2016)004).
- [44] D. A. Roberts and B. Swingle, *Phys. Rev. Lett.* **117**, 091602 (2016), URL <https://link.aps.org/doi/10.1103/PhysRevLett.117.091602>.
- [45] Z.-W. Liu, S. Lloyd, E. Y. Zhu, and H. Zhu, *Phys. Rev. Lett.* **120**, 130502 (2018), URL <https://link.aps.org/doi/10.1103/PhysRevLett.120.130502>.
- [46] C. W. von Keyserlingk, T. Rakovszky, F. Pollmann, and S. L. Sondhi, *Phys. Rev. X* **8**, 021013 (2018), URL <https://link.aps.org/doi/10.1103/PhysRevX.8.021013>.
- [47] R. Fan, P. Zhang, H. Shen, and H. Zhai, *Science Bulletin* **62**, 707 (2017), ISSN 2095-9273, URL <http://www.sciencedirect.com/science/article/pii/S2095927317301925>.
- [48] C. Asplund, A. Bernamonti, F. Galli, and T. Hartman, *J. High Energ. Phys.* **2015** (2015), URL [https://doi.org/10.1007/JHEP09\(2015\)110](https://doi.org/10.1007/JHEP09(2015)110).
- [49] N. Laflorencie, *Physics Reports* **646**, 1 (2016), ISSN 0370-1573, quantum entanglement in condensed matter systems, URL <http://www.sciencedirect.com/science/article/pii/S0370157316301582>.
- [50] M. Levin and X.-G. Wen, *Phys. Rev. Lett.* **96**, 110405 (2006), URL <http://link.aps.org/doi/10.1103/PhysRevLett.96.110405>.
- [51] A. Kitaev and J. Preskill, *Phys. Rev. Lett.* **96**, 110404 (2006), URL <http://link.aps.org/doi/10.1103/PhysRevLett.96.110404>.
- [52] H. Li and F. D. M. Haldane, *Phys. Rev. Lett.* **101**, 010504 (2008), URL <http://link.aps.org/doi/10.1103/PhysRevLett.101.010504>.
- [53] I. Peschel and V. Eisler, *Journal of Physics A: Mathematical and Theoretical* **42**, 504003 (2009), URL <https://doi.org/10.1088%2F1751-8113%2F42%2F50%2F504003>.
- [54] J. Bisognano and E. H. Wichmann, *Jour. Math. Phys.* **16**, 985 (1975), URL <https://doi.org/10.1063/1.522605>.
- [55] X. Wen, S. Ryu, and A. W. W. Ludwig, *Phys. Rev. B* **93**, 235119 (2016), URL <https://link.aps.org/doi/10.1103/PhysRevB.93.235119>.
- [56] F. Parisen Toldin and F. F. Assaad, *Phys. Rev. Lett.* **121**, 200602 (2018), URL <https://link.aps.org/doi/10.1103/PhysRevLett.121.200602>.
- [57] X. Turkeshi, T. Mendes-Santos, G. Giudici, and M. Dalmonte, *Phys. Rev. Lett.* **122**, 150606 (2019), URL <https://link.aps.org/doi/10.1103/PhysRevLett.122.150606>.
- [58] W. Zhu, Z. Huang, and Y.-C. He, *Phys. Rev. B* **99**, 235109 (2019), URL <https://link.aps.org/doi/10.1103/PhysRevB.99.235109>.
- [59] I. Peschel, *Journal of Physics A: Mathematical and General* **36**, L205 (2003), URL <https://doi.org/10.1088%2F0305-4470%2F36%2FL205>.
- [60] J. Cardy and E. Tonni, *Journal of Statistical Mechanics: Theory and Experiment* **2016**, 123103 (2016), URL <http://stacks.iop.org/1742-5468/2016/i=12/a=123103>.
- [61] X. Wen, S. Ryu, and A. W. W. Ludwig, *Journal of Statistical Mechanics: Theory and Experiment* **2018**, 113103 (2018), URL <https://doi.org/10.1088%2F1742-5468%2Faae84e>.
- [62] G. Di Giulio, R. Arias, and E. Tonni, arXiv e-prints arXiv:1905.01144 (2019), 1905.01144.
- [63] V. Eisler, E. Tonni, and I. Peschel, *Journal of Statistical Mechanics: Theory and Experiment* **2019**, 073101 (2019), URL <https://doi.org/10.1088%2F1742-5468%2Fb1f0e>.
- [64] S. R. White, *Phys. Rev. Lett.* **69**, 2863 (1992), URL <http://link.aps.org/doi/10.1103/PhysRevLett.69.2863>.
- [65] S. R. White and A. E. Feiguin, *Phys. Rev. Lett.* **93**, 076401 (2004), URL <https://link.aps.org/doi/10.1103/PhysRevLett.93.076401>.
- [66] Supplementary Materials (????).
- [67] M. A. Cazalilla, R. Citro, T. Giamarchi, E. Orignac, and M. Rigol, *Rev. Mod. Phys.* **83**, 1405 (2011), URL <https://link.aps.org/doi/10.1103/RevModPhys.83.1405>.
- [68] M. P. A. Fisher, P. B. Weichman, G. Grinstein, and D. S. Fisher, *Phys. Rev. B* **40**, 546 (1989), URL <https://link.aps.org/doi/10.1103/PhysRevB.40.546>.
- [69] T. D. Kühner and H. Monien, *Phys. Rev. B* **58**, R14741 (1998), URL <https://link.aps.org/doi/10.1103/PhysRevB.58.R14741>.
- [70] X.-L. Qi and D. Ranard, *Quantum* **3**, 159 (2019), ISSN 2521-327X, URL <http://dx.doi.org/10.22331/q-2019-07-08-159>.
- [71] Very recently, this method has been successfully applied to many different systems, such as Ref. [21, 72–76].
- [72] E. Chertkov and B. K. Clark, *Phys. Rev. X* **8**, 031029 (2018), URL <https://link.aps.org/doi/10.1103/PhysRevX.8.031029>.
- [73] M. Dupont and N. Laflorencie, *Phys. Rev. B* **99**, 020202 (2019), URL <https://link.aps.org/doi/10.1103/PhysRevB.99.020202>.
- [74] M. Dupont, N. Macé, and N. Laflorencie, *Phys. Rev. B* **100**, 134201 (2019), URL <https://link.aps.org/doi/10.1103/PhysRevB.100.134201>.
- [75] E. Bairey, I. Arad, and N. H. Lindner, *Phys. Rev. Lett.* **122**, 020504 (2019), URL <https://link.aps.org/doi/10.1103/PhysRevLett.122.020504>.
- [76] X. Turkeshi, T. Mendes-Santos, G. Giudici, and M. Dalmonte, *Phys. Rev. Lett.* **122**, 150606 (2019), URL <https://link.aps.org/doi/10.1103/PhysRevLett.122.150606>.
- [77] F. Alet and N. Laflorencie, *Comptes Rendus Physique* **19**, 498 (2018), ISSN 1631-0705, quantum simulation / Simulation quantique, URL <http://www.sciencedirect.com/science/article/pii/S163107051830032X>.
- [78] M. Dalmonte, B. Vermersch, and P. Zoller, *Nat. Phys.* **14**, 827 (2018), URL <https://www.nature.com/articles/s41567-018-0151-7>.